

# An Experimental Study on Glass Cracking and Fallout by Radiant Heat Exposure

Kazunori Harada

Dept. of Architecture and Environmental Design, Kyoto University  
Yoshida-Honmachi, Sakyo, Kyoto, 606-8501, Japan

Atsushi Enomoto, Kazuki Uede and Takao Wakamatsu

Dept. of Architecture, Science University of Tokyo  
Yamasaki 2641, Noda, Chiba, 278-8510, Japan

## ABSTRACT

To develop a simple model to predict the glass cracking and/or breaking, radiant heating tests were carried out on float glass and wired glass. By changing the imposed heat flux and lateral restraint of the glass, 50 experiments were carried out to measure the time to initial crack and fallout. Temperatures were measured at the center of glass pane and edge, while the strain was measured at the edge. From the experimental data, the critical heat flux was determined under which no glass cracking takes place. By using the measured temperature and stress, the ultimate tensile stress of the glass edge was calculated. The obtained values were lower than the literature values for plain glass surface where no effect of micro defects at the cutting edge is taken into account. By analysing the post crack behavior, it was pointed out that the fallout area mainly depends on imposed heat flux and slightly on restraint. Under intense heating (more than  $9\text{kW/m}^2$ ), large piece of glass tends to fall out, however under moderate heating, glass just cracks but did not fall out. Therefore it was pointed out that the application of the thermal stress model for glass breaking is limited to intensely heated scenarios. A simple prediction formula was derived for such scenarios.

**Key words:** initial crack, thermal stress, ultimate tensile stress, critical heat flux, fallout

## INTRODUCTION

Glass breaking causes drastic changes in fire development. In the room of fire origin, glass breaking increases the air supply to the fire room, which often increases fire development such as flashover. In the fully developed stage, fire spreads through the broken window glass. As has been pointed out, the needs for modeling glass breaking is obvious.

Several engineering models were already proposed based on thermal stress theory<sup>1-4</sup>. In these models, temperature profile is calculated by heat conduction coupled with radiant absorption and emission in the glass. The resulting temperature profile is used to calculate the thermal stress (tensile at the edge) to compare with ultimate tensile stress of the glass in order to evaluate the onset of cracking at the glass edge. The criteria for crack initiation often appears as, (refer to nomenclature for symbols)

$$\sigma_E = f' \alpha E (T_G - T_E) > \sigma_{E,ult} \quad (1)$$

It is recognized that the above approach is successful<sup>5</sup>. However two aspects are to be examined. (1) The glass properties, especially the ultimate tensile stress  $\sigma_{E,ult}$ , range considerably. Thus there is a need for collecting data. (2) Glass cracking is a trigger of glass fallout. However the actual fallout sometimes does not take place. Thus the application of the crack model may be limited.

In this study, a series of experiments was carried out. Two types of glass (float glass and wired glass) were heated by radiation to collect the data for ultimate tensile stress. Also the post-crack behavior was observed and correlated with radiation levels and degree of restraint.

## EXPERIMENTAL CONDITION

### Apparatus

The testing apparatus is shown in FIGURE 1. A specimen was put in front of a propane-fired radiant panel. The imposed heat flux was varied in the range of 3 to 10 kW/m<sup>2</sup> by changing the distance between the radiant panel and specimen. Before starting a test, radiation shield was put in front of the specimen. After the radiant panel was heated up, the shield was removed, which results in stepwise heating of the specimen at constant radiation heat flux. FIGURE 2 shows the experimental situation.

Using two infra-red thermometers, the glass pane temperature was measured at the center of the glass by viewing from exposed and unexposed side of the specimen. A heat flux gauge was equipped 100mm below the specimen in order to monitor the imposed heat flux. Surrounding temperatures at both sides were measured by thermocouples shielded by aluminum tube.

### Specimens

The specimens were non heat-treated ordinary float glass (3mm thick) and parallel wired glass (6.8mm thick, 50mm wire pitch). The detail of the specimen is shown in FIGURE 3. The glass was a 500mm squared plate with 15mm shaded length. The glass was supported by two rubber blocks at bottom edge. Some of the specimens were given lateral restraint by the other two blocks placed at side edges. At the center of all the edges, strain gauges and thermocouples were placed. Table 1 summarizes the experimental conditions. Total number of specimens were 50, differing in glass type, lateral restraint and imposed radiation.

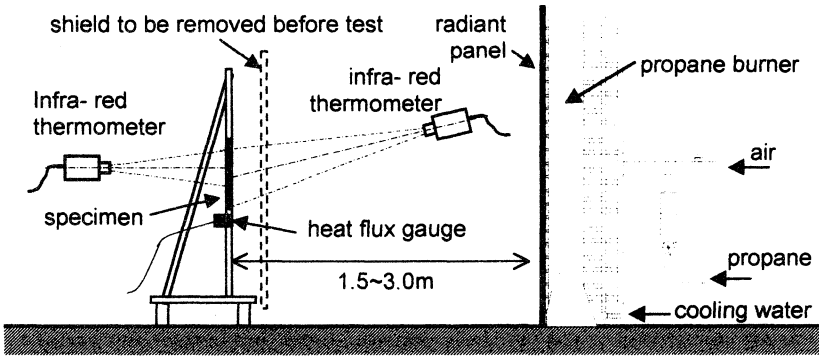


FIGURE 1 Experimental Apparatus

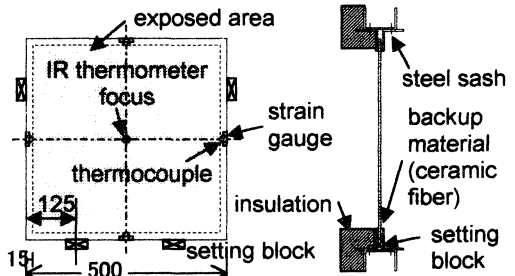
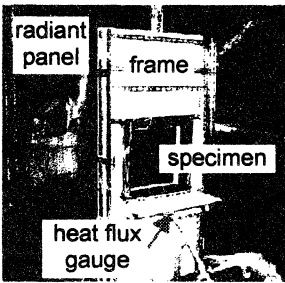
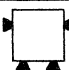





FIGURE 2 View of the Experiment      FIGURE 3 Specimen Details

TABLE 1 Summary of Experimental Conditions

glass type and restraint	imposed heat flux [ $\text{kW/m}^2$ ]	number of tests
 float glass (3mm) with lateral restraint	low / 5.5 (5.5-5.5)	3
	medium / 6.7 (6.4-6.9)	3
	high / 9.1 (8.7-9.6)	3
 float glass (3mm) without lateral restraint	low / 5.5 (2.85-5.72)	10
	medium / 7.4 (6.83-8.22)	8
	high / 9.1 (9.02-9.23)	3
 wired glass (6.8mm) with lateral restraint	low / 2.8 (2.7-3.0)	3
	medium / 5.4 (5.3-5.5)	3
	high / 9.5 (9.0-9.9)	3
 wired glass (6.8mm) without lateral restraint	low / 2.8 (2.8-2.9)	5
	medium / 5.4 (5.2-5.5)	3
	high / 9.5 (9.4-9.7)	3

## EXPERIMENTAL RESULTS

As an example, the results of test No. 10 (float glass without lateral restraint, imposed heat flux  $7.03\text{ kW/m}^2$ ) is shown in FIGURE 4. In the early stage, glass pane temperature rises rapidly, while the edge temperature rise is slow. At 160 seconds, cracking took place. Two small pieces of glass fell out almost at the same time. Strain is monotonically increased with time until initial crack, followed by a sudden decrease. All the results are summarized in Tables 2 and 3, categorized by glass type, restraint and level of imposed heat flux.

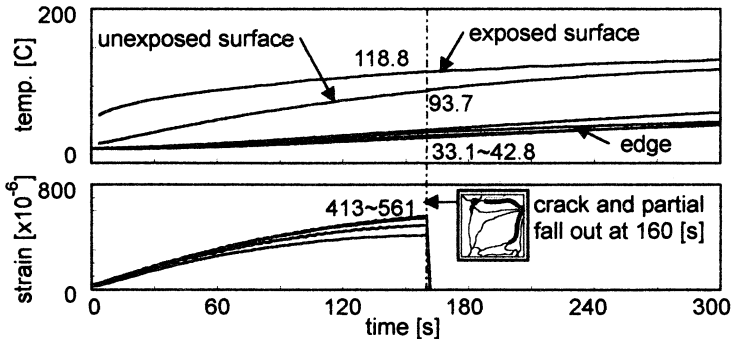


FIGURE 4 Results of Test No.10 (float glass, no lateral restraint, heat flux =  $7.03\text{ kW/m}^2$ )

### ANALYSIS OF INITIAL CRACK BEHAVIOR

Experimental data was analyzed for the initial crack condition. Correlation was established between experimental parameters (glass type, imposed heat flux and degree of restraint) and initial crack behavior (time to initial crack, ultimate tensile stress, geometrical factor).

#### Time to Initial Crack

The time to initial crack is plotted in FIGURE 5 as functions of imposed heat flux. Both in float and wired glass, the dependence is clear. As the flux increases, the time to initial crack decreases gradually. There is a certain threshold of the heat flux necessary for glass cracking (critical heat flux, hereafter). The value is approximately  $5.0\text{ kW/m}^2$  for float glass,  $2.0\text{ kW/m}^2$  for wired glass.

The difference by glass type is obvious. Wired glass is much easier to crack than float glass. This is due to the micro defects at the glass edge developed during glass cutting process. As the wired glass is hard to be cut, many defects would exist at the cutting edge even before heating. These defects might be the crack initiation points. The difference by lateral restraint is not clear on the time to initial crack.

TABLE 2 Summary of Experimental Results (float glass, 3mm)



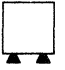

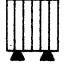
run No.	glass type and restraint	imposed heat flux [kW/m <sup>2</sup> ]	at initial crack					time to fall out [s]	final fall out area [%]	
			time to crack [s]	edge strain [ $\times 10^{-6}$ ]	pane temp. [°C]	edge temp. [°C]	temp. difference [K]			
1	float glass (3mm) with lateral restraint 	5.43	172	400	80.3	35.5	44.8	-	0	
2		low	5.50	214	412	86.6	43.5	43.2	-	0
3			5.50	234	448	90.9	42.9	48.0	234	0.7
7		med.	6.41	170	511	92.9	36.5	56.4	170	1.2
8			6.73	124	460	83.0	31.9	51.1	166	0.3
9			6.92	138	488	88.8	36.3	52.5	-	0
16		high 	8.72	74	415	82.9	32.3	50.6	-	0
17			8.99	108	505	102.9	38.4	64.5	108	17.0
15			9.63	88	480	94.2	35.6	58.6	88	7.5
24	float glass (3mm) without lateral restraint 	2.85	no crack					-	0	
25		3.10	no crack					-	0	
26		3.55	no crack					-	0	
27		4.10	no crack					-	0	
28		4.65	no crack					-	0	
29		4.85	no crack					-	0	
5		low	5.31	218	427	87.8	44.6	43.2	218	0.1
30	5.41		272	404	88.0	45.7	42.3	272	0.4	
4	5.62		204	422	100.7	56.5	44.2	204	2.0	
6	5.72		376	399	104.8	48.9	56.0	376	4.5	
14	med.	6.83	106	371	76.0	32.4	43.6	190	0.7	
10		7.03	160	503	93.7	37.9	55.8	160	1.2	
13		7.16	156	510	94.3	37.5	56.8	156	0.8	
12		7.18	144	482	90.0	35.8	54.2	-	0	
11		7.24	142	498	91.8	39.4	52.4	142	0.2	
18		7.78	80	448	79.1	29.8	49.3	80	0.8	
23		7.80	132	673	100.6	32.0	68.6	252	1.1	
22		8.22	104	504	98.8	39.5	59.3	-	0	
19	high	9.02	68	418	77.3	29.3	48.0	220	0.7	
20		9.03	78	443	89.3	39.8	49.4	78	5.3	
21		9.23	96	524	99.0	40.7	58.3	96	24.0	

TABLE 3 Summary of Experimental Results (Wired Glass, 6.8mm)

run No.	glass type and restraint	imposed heat flux [kW/m <sup>2</sup> ]	at initial crack					time to fall out [s]	final fall out area [%]	
			time to crack [s]	edge strain [ $\times 10^{-6}$ ]	pane temp. [°C]	edge temp. [°C]	temp. difference [K]			
32	wired glass (6.8mm) with lateral restraint	low	2.74	270	176	43.9	22.9	21.0	-	0
33			2.78	300	174	46.9	27.4	19.5	-	0
31			2.96	300	192	48.9	26.4	22.5	-	0
39	with lateral restraint	med.	5.31	102	187	46.7	24.0	22.7	-	0
40			5.38	102	193	40.1	17.6	22.6	-	0
38			5.53	98	191	42.8	22.0	20.8	-	0
46		high	8.99	58	203	47.9	25.6	22.3	-	0
45			9.65	44	139	43.8	23.3	20.5	-	0
44			9.90	48	176	44.7	22.7	22.0	-	0
35	wired glass (6.8mm) without lateral restraint	low	2.83	no crack					-	0
35			2.83	298	data not available					-
36		2.83	318	177	48.3	28.8	19.5	-	0	
34		2.84	284	162	45.1	27.2	18.0	-	0	
37		2.87	272	154	47.8	27.7	20.1	-	0	
42		with lateral restraint	med.	5.21	152	240	54.9	28.0	26.9	-
41	5.34			102	183	44.6	23.5	21.1	-	0
43	5.50			106	182	45.6	23.6	22.0	-	0
48		high	9.36	64	219	49.0	23.7	26.9	-	0
47			9.40	54	182	45.7	22.9	22.8	-	0
49			9.67	50	172	47.7	24.6	23.2	-	0

In the following, a simplified model is proposed to calculate the time to initial crack under constant heat flux. The model intends to be simple enough and conservative in order to be used in building design process.

The heat balance of the glass pane and edge would be,

$$c\rho V_G \frac{dT_G}{dt_G} = q - A_G h(T_G - T_0). \tag{2}$$

If the imposed heat flux  $q$  is constant over time, equation (2) can be integrated analytically to result in

$$t = \left(\frac{c\rho d}{2h}\right) \log_e \left(\frac{q}{q - 2h(T_G - T_0)}\right). \tag{3}$$

At the critical condition for cracking, the rate of heat loss from glass surfaces is equal to the imposed heat flux,

$$q_{crit} = 2h(T_G - T_0) \Big|_{at\ crack} \tag{4}$$

Thus we get,

$$t_{crack} = \left( \frac{c\rho d}{2h} \right) / \log_e \left( \frac{q}{q - q_{crit}} \right) \tag{5}$$

Referring to the experimental data, the critical heat flux was selected as 5 and 2 for float and wired glass. The solid curves in FIGURE 5 were plotted by equation (5) with  $\rho=2500[\text{kg/m}^3]$ ,  $c=0.92[\text{kJ/kg.K}]$ ,  $h=0.04[\text{kW/m}^2.\text{K}]$ , which results in reasonable agreement.

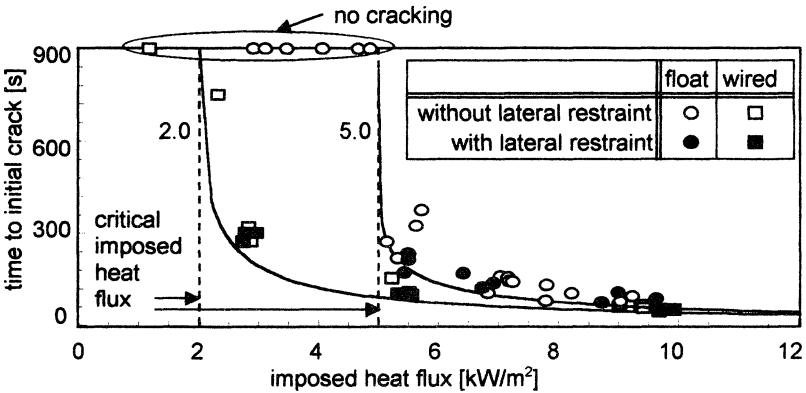


FIGURE 5 Time to Initial Crack as Functions of Imposed Heat Flux

**Glass Properties Associated with Initial Crack**

If the imposed radiation varies with time, the heat balance equation is to be integrated numerically to calculate the edge stress. The resultant stress is compared with ultimate stress. For this purpose, two glass properties, tensile strength and geometrical factor, were derived from measured quantities.

Tensile Strength of Glass Edge

Using the data at initial crack, the ultimate tensile stress of the glass edge was derived. As shown in FIGURE 6, we approximated that the glass pane and edge expands in parallel to its perimeter. Then the free thermal strain would be,

$$\varepsilon_{G,th} = \alpha(T_G - T_0) \quad (6)$$

$$\varepsilon_{E,th} = \alpha(T_E - T_0), \quad (7)$$

at the pane and edge, respectively. To fulfil the difference in free thermal strain, the edge would be forced to expand. The resultant stress- related strain would be  $(\varepsilon_{G,th} - \varepsilon_{E,th})$ . Thus the tensile stress could be written,

$$\sigma_E = E(\varepsilon_{G,th} - \varepsilon_{E,th}) = E(\varepsilon_{E,tot} - \varepsilon_{E,th}). \quad (8)$$

From the experimental data, the total strain  $\varepsilon_{E,tot}$  and edge temperature  $T_E$  are available. Rearranging the equations (6)-(8), the ultimate tensile stress could be expressed using measured quantities at initial crack,

$$\sigma_{E,ult} = E(\varepsilon_{E,tot} - \alpha(T_E - T_0)) \Big|_{at\ crack}, \quad (9)$$

where the modulus of elasticity  $E=730$ [MPa] and coefficient of linear expansion  $\alpha=8.75 \times 10^{-4}$  [K<sup>-1</sup>] were used in the calculations.

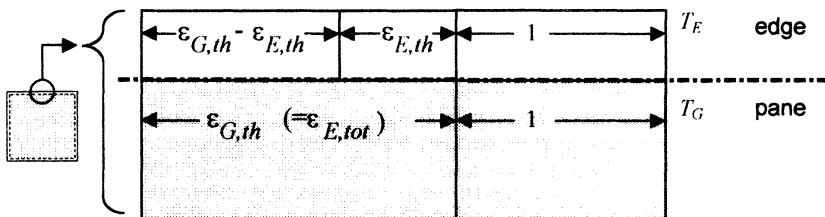


FIGURE 6 Thermal Stress by non Uniform Temperature Profile between Pane and Edge

The results for float glass are summarized in FIGURE 7 in terms of cumulative distribution function categorized by the level of imposed heat flux (low, medium, high). In case of float glass, the ultimate stress is in the range of 15 to 35 [MPa]. As the heat flux is increased, the ultimate stress tends to be increased slightly. Also plotted in FIGURE 7 are the literature values for bending<sup>2)</sup> and punching<sup>6)</sup> failure. These values are higher than the present data, because the breaking in these failure modes corresponds with the strength of the smooth glass surface. In contrast, the present data corresponds with edge strength including the effect of small defects on the cutting edge.

The results for the wired glass are shown in FIGURE 8. The ultimate stress is in the range of 3 to 13 [MPa], which is about one third of the float glass. This implies additional defects around the embedded wires compared with float glass.



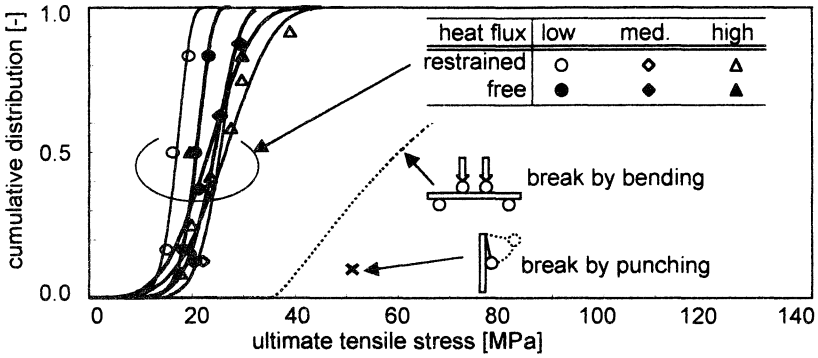


FIGURE 7 Ultimate Tensile Strength of Glass Edge (Float Glass, 3mm thick)

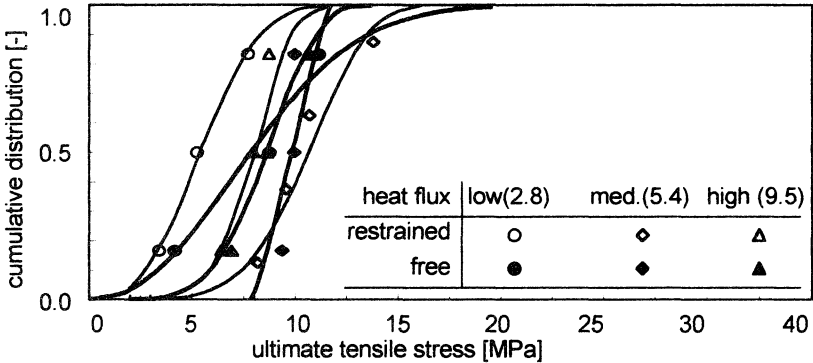


FIGURE 8 Ultimate Tensile Strength of Glass Edge (Wired Glass, 6.8mm thick)

**Geometrical Factor:**

In the evaluation of tensile stress, geometrical factor (sometimes called edge coefficient),  $f'$ , is often preferred. From the experimental data, the factor was calculated by

$$f' = \sigma_{E,ult} / \alpha E (T_G - T_E) \Big|_{at\ crack} \tag{10}$$

The results are summarized in FIGURE 9, in category of glass type and the level of imposed heat flux. In case of float glass. The factor ranges in 0.6 and 0.73 (float glass) or in 0.53 to 0.68 (wired glass). Even the value has some scatter, the conventional value ( $f'=0.65$ ) gives a good estimate of the geometrical factor.

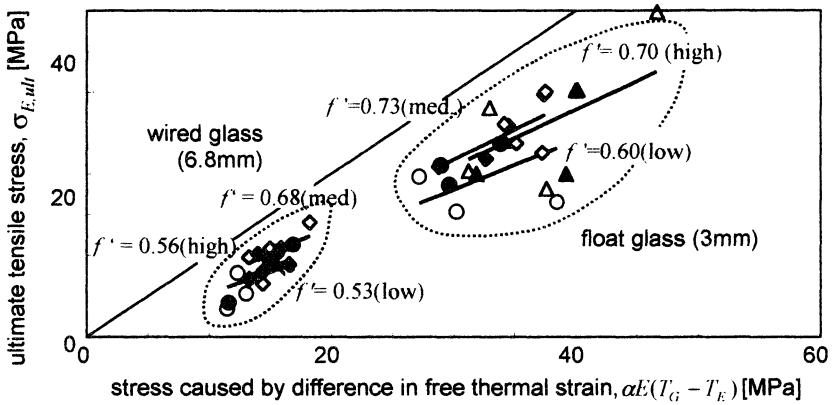


FIGURE 9 Geometrical Factor  $f' = \sigma_E / \alpha E(T_G - T_E)$  (see FIGURE 7 for symbols)

### ANALYSIS OF POST CRACK BEHAVIOR

During the experiments, crack development and fall out patterns were observed by eye. The results are summarized below for the time to fall out and final fall out area.

**Float glass:** The increase of the fallout area with time is plotted in FIGURE 10. For most of the tests, small pieces of the glass fell out at the same time as initial crack. However in some of the tests, large pieces of glass fell out successively. This occurred under large imposed heat flux over  $9 \text{ kW/m}^2$ . The tendency is clear in FIGURE 11, where the fraction of final fallout

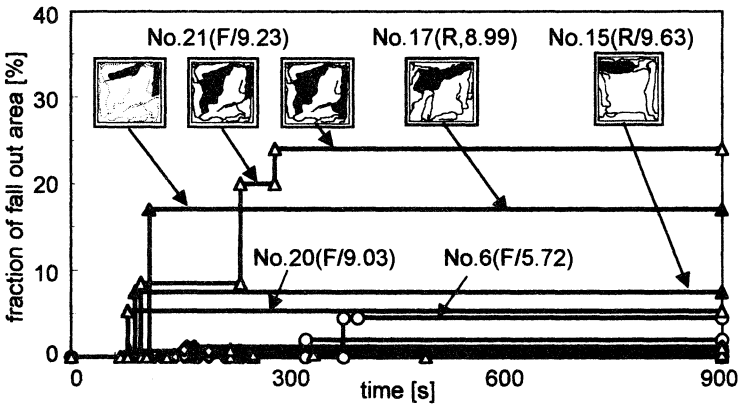


FIGURE 10 Increase of the Fallout Area with Time (F= not restrained, R= restrained, numeric values = imposed heat flux in  $\text{kW/m}^2$ )

area was plotted against imposed heat flux. In cases of imposed flux less than  $9 \text{ kW/m}^2$ , the fallout area remains small, which means that the initial crack does not trigger the fallout of large pieces of glass. It can also be pointed out that the lateral restraint tends to reduce the glass fallout compared with non restrained glass.

**Wired glass:** Typical final crack patterns for wired glass is shown in FIGURE 12. It is clear that the crack is intensified as the imposed heat flux is increased. However no fallout was observed because of the benefit of wires embedded in the glass. The difference by lateral restraint is not clear in this result.

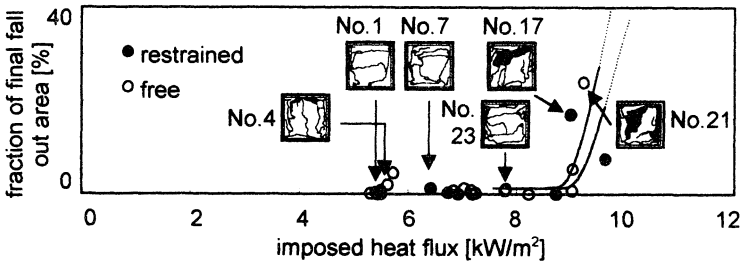


FIGURE 11 Final Fallout Area (fraction) of 3mm Float Glass

restraint	imposed heat flux		
	Low	medium	high
laterally restrained	No.32( $2.7 \text{ kW/m}^2$ ) 	No.40( $5.4 \text{ kW/m}^2$ ) 	No.44( $9.9 \text{ kW/m}^2$ ) 
free	No.35( $2.8 \text{ kW/m}^2$ ) 	No.41( $5.3 \text{ kW/m}^2$ ) 	No.48( $9.4 \text{ kW/m}^2$ ) 

FIGURE 12 Final Crack Pattern of 6.8mm Wired Glass

**CONCLUSIONS**

The glass cracking and subsequent fallout were observed by experiments. The glass type, lateral restraint and imposed heat flux were varied between experiments. The results on initial crack behavior are:

- The ultimate tensile stress was in the order of 25[MPa] for non heat treated float glass, 10 [MPa] for wired glass.
- The restraint of the glass have almost no effect on glass cracking.

By analysing the post crack behavior, it was pointed out that :

- Post crack behavior of the glass depends on imposed heat flux and restraint. Under intense heating (more than  $9[\text{kW/m}^2]$ ), large pieces of glass tend to fall out.
- Restraint seems to reduce the fallout of glass pieces to a certain degree.

## ACKNOWLEDGEMENTS

The authors would like to thank Mr. Asano and Mr. Sanou (formerly the Science University Students) for their elaborate experimental work. The experimental work was carried by using the radiant panel facility in Building Research Institute. The financial support by Science and Technology Agency for this project is acknowledged.

## NOMENCLATURE

### Alphabets

$A$	area [ $\text{m}^2$ ]	$l$	perimeter length [m]
$c$	specific heat [ $\text{J/kg}\cdot\text{K}$ ]	$q$	imposed heat flux [ $\text{kW/m}^2$ ]
$d$	glass thickness [m]	$t$	time [s]
$E$	modulus of elasticity [MPa]	$T$	temperature [K]
$f'$	geometrical factor [-]	$V$	volume [ $\text{m}^3$ ]
$h$	convective coefficient [ $\text{W/m}^2\cdot\text{K}$ ]		
$k$	thermal conductance [ $\text{kW/m}^2\cdot\text{K}$ ]		

### Greek letters

$\alpha$	coeff. of linear expansion [ $\text{K}^{-1}$ ]	$\rho$	density [ $\text{kg/m}^3$ ]
$\varepsilon$	strain [-]	$\sigma$	stress [MPa]

### Subscripts

G	glass pane	ult	ultimate
E	glass edge	crit	critical
st	stress- related	0	ambient
th	thermal		

## REFERENCES

1. Keski-Rahkonen, O., "Breaking of Window Glass Close to Fire", *Fire and Materials*, 12, pp. 61- 69, 1988 and 15, pp. 11-16, 1991
2. Joshi, A., A., Pagni, P., J., "Fire- Induced Thermal Fields in Window Glass I- Theory, II- Experiments", *Fire Safety Journal*, 22, pp. 25-43 and 45- 65, 1994
3. Virgone, J., Depecker, P., Krauss, G., "Computer Simulation of Glass Temperatures in Fire Conditions", *Building and Environment*, 32(1), pp.13-23, 1997
4. Sincaglia, P. E. and Barnett, J. R., "Development of a Glass Window Fracture Model for Zone-Type Computer Fire Codes," *Journal of fire Protection Engineering*, Vol. 8, pp.101-118, 1997.
5. Mowrer, F., W., *Window Breakage Induced by Exterior Fires*, NIST-GCR-98-751, National Institute of Standards and Technology, Gaithersburg, 1998.
6. Kenchiku Bousai Kyokai, *Safety Design of Glass Openings*, 1991 (in Japanese)